Vietnam Journal of Science and Technology ***57*** *(3A) (2019) 1-10*
doi:10.15625/2525-2518/57/3A/13936

ANTIBACTERIAL AND PHOTOCATALYTIC ABILITY OF THE Ag/TiO_2 COATING ON THE GLASS SURFACE

Do Quang Minh, Dao Thi Thuy Hong, Nguyen Ngoc Tuong Vi

Ho Chi Minh City University of Technology - VNU-HCM, 268 Ly thuong Kiet street, 10 district, Ho Chi Minh City

*Email: mnh_doquang@yahoo.com

Received: 12 July 2019; Accepted for publication: 5 September 2019

Abstract. The coating on the glass surface was made by heating the mixture of Ag resinate and tetra-n-butyl orthotitanate (TBO) at 570 ^oC for 1 hour. The characteristics and structure of the mixture of Ag/TiO_2 with the content of Ag : TiO_2 from 0 – 8 (% mol.) were studied by the methods such as XRD, FTIR, UV-vis, SEM, EDS. The research results of antibacterial ability and the degradation of blue methylene (MB) were shown that this coating can be used for antibacterial and photocatalytic ability.

Keywords: coating on the glass surface, Ag/ TiO_2, antibacterial, photocatalytic ability.

Classification numbers: 2.2.3, 3.7.1, 3.7.3.

1. INTRODUCTION

Titanium oxide (TiO_2) has been widely studied for photocatalytic degradation of harmful organic pollutants from the wastewater due to its nontoxicity. Because of the bandgap energy (E_g) in the range 3.2 ÷ 3.4 eV, its natural visible light absorption efficiency, photocatalytic efficiency and practical applicability would be limited. To enhance the photocatalytic ability of TiO_2, the noble metals such as Pt, Pd, Rh, Au, and Ag are often used [1]. The noble metals are having the superior photocatalytic ability but their high cost limits their scale applications. Among them, Ag is the less expensive and can be used as a visible sensitive material for photocatalytic activity. Ag can replace Ti in the crystal structure of TiO_2, thus its Eg would be reduced and the natural visible-light absorption would be extended. Ag can also be dispersed on the surface of TiO_2 crystals and Ag/TiO_2-based composite could be created. In the Ag/TiO_2 composite, Ag nanoparticles receive excited electrons from semiconductors TiO_2, facilitating the reduction of dioxygen and thus the Ag/TiO_2 composite exhibit enhanced UV light catalytic activity to decompose organic substances. Using different amounts of the Ag metal nanoparticles on the surface of semiconductors TiO_2 can be an effective way to improve photocatalytic activity [2, 3].

There are many methods of doping Ag into TiO_2, as known as TiO_2 modify, such as the hydrothermal method [4, 5], radiation by γ-ray [6], sol–gel method [7, 8], precipitation in solution thermal decomposition, etc. The method of doping TiO_2 by thermal decomposition of the mixture of Ag resinate and tetra-n-butyl orthotitanate ($Ti(OCH(CH_2)_2)_4$ on a glass surface is

presented in this paper. The tetra-n-butyl orthotitanate ($Ti(OCH(CH_2)_2)$ is a Chinese chemical, and from here it will be denoted by TBO. The Ag resinate is a product made from coconut oil. The glass with this coating can be used for the antibacterial and photocatalytic material.

2. THE EXPERIMENTAL PROCEDURE

2.1. Raw materials

The Ag resinate was prepared from $AgNO_3$ and the coconut oil. The coconut oil is composed mainly of medium-chain saturated fatty acids called medium-chain triglycerides, they will be denoted by RCOOH. In the coconut oil, lauric acid ($CH_3(CH_2)_{10}COOH$) is about accounting for 47.5% weight. Firstly, the acidity of the coconut oil has been titrated to calculate the amount of NaOH required for the saponification reaction (according to the TCVN 6127:2010). In the saponification reaction, the ratio of 50 mL of NaOH 0.5M solution with 5 g of the coconut oil was used. The product of this reaction is solid soap Na (denoted by RCOONa). Then let $AgNO_3$ react with RCOONa to form Ag resinate (RCOOAg) with a molar ratio of RCOONa : $AgNO_3$ = 1:1. The reactions can be summarized as follows:

$$RCOOH + NaOH = RCOONa + H_2O$$

$$RCOONa + AgNO_3 = RCOOAg + NaNO_3$$

The powder of the Ag resinate (RCOOAg) was washed and mixed with TBO at the required rate, that was calculated by 0 – 8 (% mol) of Ag/TiO_2. These mixtures were decomposed at high temperatures to create the Ag/TiO_2 composite. Analytical methods as Fourier transform infrared spectrometer (FTIR), differential thermal scanning (DSC), thermal gravity analysis (TGA), X-ray diffraction (XRD), scanning electronic microscopy (SEM), Energy-dispersive X-ray (EDS) were used to detect the doping Ag into TiO_2 and the characteristics of the Ag/TiO_2 composite.

2.2. The physical characteristics of composite Ag/TiO_2

Chemical compositions of used glass are (% wt.): 72.39 SiO_2; 1.39 Al_2O_3; 0.125 Fe_2O_3; 9.17 CaO; 3.13 resinate reaction and the formation of the Ag/TiO_2 composite were evaluated according to the MgO; 13.29 Na_2O (others 0.505) and its softening temperature is about 600 ^oC. At temperatures less than 600 ^oC, the glass plates are not deformed. At temperatures close to this temperature the organic substances have been decomposed, inorganic substances will be created the stable coatings on the glass surfaces.

The effects of the forming bonds by FTIR. The FTIR samples were prepared as KBr pellets, by using a device Thermo Fisher Scientific.

The crystal structure and interaction of the Ag resinate (RCOOAg) with the TBO were investigated by XRD. The change of lattice parameters of TiO_2 crystal (tetragonal unit cell) may be calculated according to the formula:

$$\frac{1}{d^2} = \frac{h^2 + k^2}{a^2} + \frac{l^2}{c^2} \qquad (2.1)$$

where a, c, d are lattice parameters, (hkl) are Miller indices.

The heating temperatures of the samples were detected by DSC and TGA with a device Metter Toledo. The heating temperatures must ensure that the organic substances are completely decomposed, the glass is not deformed and the coating adheres firmly to the glass surface.

The bandgap E_g of the samples was characterized by UV/Vis spectroscopy (Lambda 950 spectrophotometer). E_g was estimated according to the Tauc's formula and the Tauc's plot. After that, E_g is determined by the intersection point between the linear interpolation line of the graph and the E_g axis [9].

$$h\nu = \frac{A(h\nu - E_g)^n}{\alpha} \tag{2.2}$$

where h is Planck's constant, h = 6.626×10-34 [J.s] = 4.137× 10-15 [eV.s]; α is the absorption coefficient; ν is the frequency and n is a constant (n = ½ for non-direct E_g and n = 2 for directly E_g. In this case, n = ½ for anatase).

2.3. Antibacterial and photocatalytic ability of the Ag/TiO_2 coating on the glass surface

The mixture of the Ag resinate with the TBO and glass powder was dispersed in the commercial solvent C8720 (Carpoly) and covered on the surface of the glass plates with sizes 2×3 (cm) or the glass powder with dimension through a 125 μm sieve (Table 1). After that, they had been heated at 570 ^oC for 1 hour. The heating temperature of 570 ^oC (< 600 ^oC - the glass softening temperature) was chosen from the results obtained on the DSC and TGA curves.

Table1. The mixing ratio in the samples M0, M4 and M8.

Sample	$ratio(mol)$ $n_{Ag}: n_{TiO_2}$	Ag resinate (g)	TBO (g)	C8720 (g)	Glass powder (g)
M0	0 : 100	0.000	0.14	8	16.29
M4	4 : 100	0.005	0.14	8	16.29
M8	8 : 100	0.010	0.14	8	16.29

The photocatalytic ability of the coating Ag/TiO_2 was detected by the degradation of Methylene Blue (MB). The MB has been chosen because it is a popular stable organic dye. In this experiment, the glass was crushed to powder with size passed through a sieve 125 μm. The samples were coated on the surface of the glass powder for the photocatalytic tests.

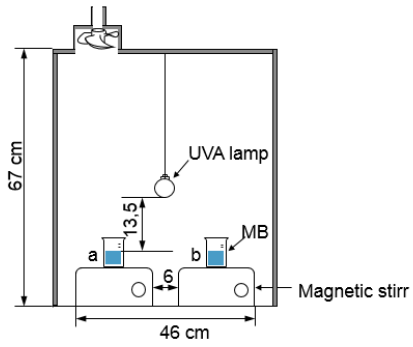

Figure 1. The experimental diagram of decomposition MB in the box with UVA lamp.

The experimental diagram is shown in Figure 1. In this experiment, two glass beakers containing 5 mg/L MB solution (96 %) were placed in a sealed box, the glass powder with the Ag/TiO_2 coating was put in one beaker (denoted b in the Fig. 1). Turn on the light by the 50W UV lamp (REPTIZOO) for 120 minutes. In the time shining both two glass beakers were stirred by the magnetic stirrer (IKA C-MAG HS) at a speed of 250 rounds/min.. After that, MB solutions were centrifuged and compared the MB concentration in both two beakers to know the photocatalytic effect of the Ag/TiO_2 coating.

The antibacterial ability of the Ag/TiO_2 coating was tested according to the ISO 20776-1: 2006 against *E. coli ATCC 25922*. Firstly, the test samples containing E. coli had been prepared. Then, the solutions contain antibacterial agents (the glass powder with the Ag/TiO_2 coating) were also prepared. The solutions with different concentrations of the antibacterial agents were mixed into Mueller-Hinton agar plates. These agar plates were cured at 37 ^oC for 20 h under the shining of a compact lamp. After that, the antibacterial ability was estimated and recorded by naked eyes. These tests were performed by doctors of HCMC University of Medicine and Pharmacy.

3. THE RESULTS OF EXPERIMENTS

3.1. FTIR spectra of coconut oil, Na soap and Ag resinate

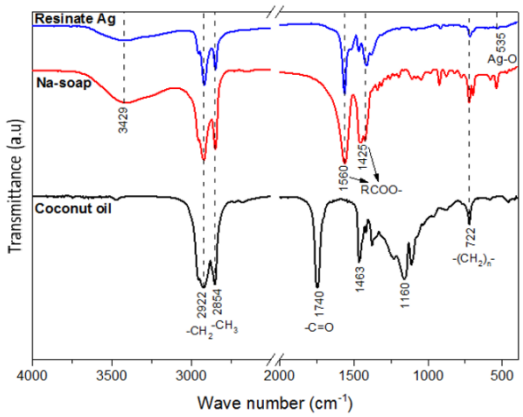

Figure 2. FTIR spectra of coconut oil, Na soap and Ag resinate.

The chains. The broadband located at 1740 cm^1 on the FTIR spectrum of the coconut oil is characterized by the organic acids and ester – C=O. It was shifted to 1560 cm^{-1} on the FTIR curves of molecular structure of the three samples (the coconut oil, Na soap and the Ag resinate) was investigated by FTIR. These FTIR spectra are shown in Figure 2.

In Figure 2, the peaks located at 2922 cm^{-1}, 2854 cm^{-1} and 722 cm^{-1} can be characterized as asymmetric stretching vibrations of bonds $–CH_2$, $–CH_3$ and $– (CH)_n –$ (with $n > 3$) [10]. Thus the reactions did not occur in hydrocarbon the Na soap and the resinate Ag [11]. That means the reaction has occurred with the organic acids. The peak at 535 cm^{-1} corresponds to the vibration of Me – O (Me: Na or Ag) [12, 13], it evidenced by forming the Na soap and the Ag resinate.

3.2. The DSC and TGA curves of the mixture of Ag resinate and TBO (Ag/TiO_2 = 4 % mol.)

Figure 3 shows the DSC and TGA curves of the mixture of the Ag resinate and the TBO (ratio of Ag/TiO_2 = 4 % mol.). It can be seen on the TGA curve, from the temperatures of T > 400 ^oC, the weight of the sample has not been changed. In other words, the organic substances have completely decomposed. On the DSC curve, there are three thermal effects. The first is the endothermic effect (from 386.75 to 430.81 ^oC), it corresponds to the melting of the inorganic substances from the mixture. The second (487 – 500 ^oC) and third (567 – 580 ^oC) effects are related to the crystallization effect and change of polymorphism of TiO_2.

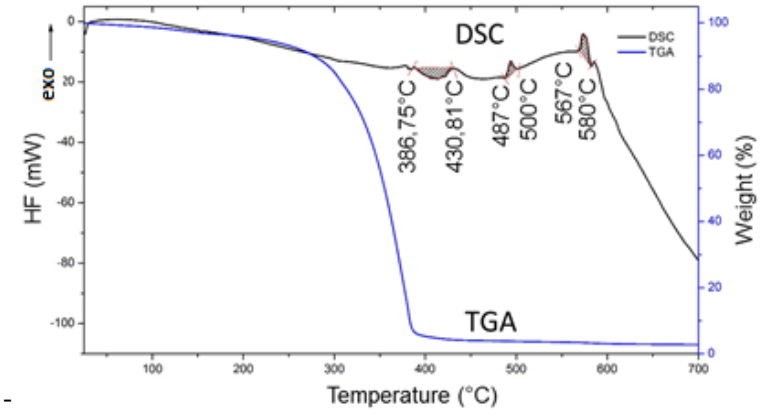

Figure 3. The DSC and TGA curves of the mixture of Ag resinate and TBO (ratio Ag/TiO_2 = 4 % mol.).

3.3. XRD, FTIR spectra of of the mixture of Ag resinate and TBO

Resinate Ag and TBO were mixed according to the ratios of 0, 4 and 8 (% mol Ag/TiO_2). These samples were denoted by M0, M4, and M8. They were fired at 570 ^oC for 1 h, then were cooled quickly in water and were analyzed by XRD. The XRD spectra are shown in Figure 4.

On the XRD spectra, compared with standard spectra [14, 15, 16] the crystalline phases of anatase (denoted A) and silver (denoted Ag) were detected. This is consistent with the DSC analysis results. Rutile (denoted R) only appears very little on the M0 sample spectrum (without Ag). Thus, it is possible that Ag prevented crystallization of the rutile.

From diffraction peaks on the XRD spectrum, the change of lattice parameters of anatase crystal (tetragonal unit cell) may be calculated and the results are shown in Table 2. The results in the Table 2 indicate that when the Ag content increases the distance between the families $d_{(200)}$ increases, while the $d_{(101)}$ decreases. At the same time, the lattice parameters *a* increase, while *c* decreases. In Table 2 it is also shown E_g of the samples M0, M4, M8.

Table 2. The change of lattice parameters and Eg of the samples M0, M4, M8.

Sample	$d_{(101)}$ (Å)	$d_{(200)}$ (Å)	a (Å)	c (Å)	E_g (eV)
M0	3.502	1.887	3.773	9.403	3.256
M4	3.499	1.892	3.786	9.188	3.120
M8	3.489	1.894	3.787	8.970	3.285

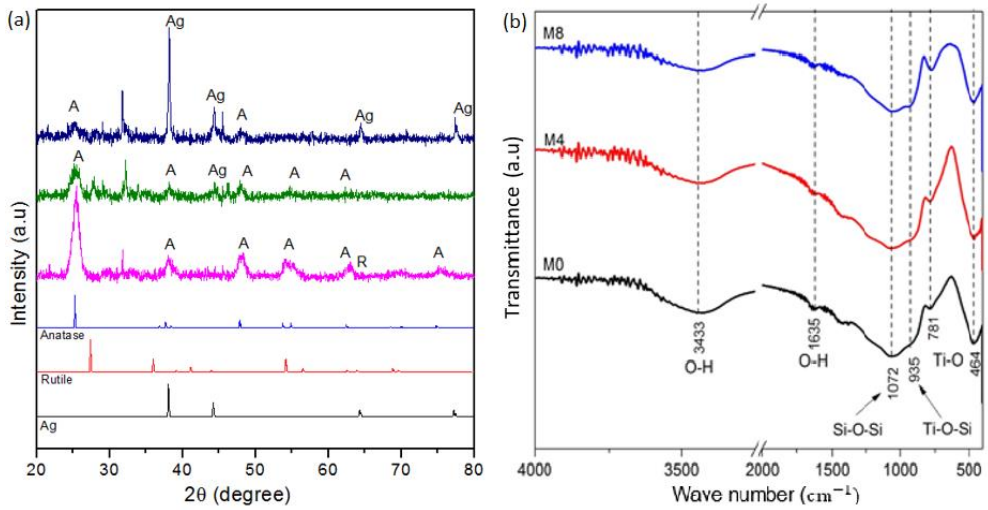

Figure 4. XRD pattern (a) and FTIR spectra (b) of the mixture of Ag resinate and TBO (the ratio of Ag/TiO_2 = 0, 4 and 8 % mol.).

On Figure 4, broadbands located at 3433 cm^{-1} and at 1635 cm^{-1} are characterized of stretching vibration and bending vibration of – OH, respectively. The peaks at 1069 cm^{-1} is characterized of Si-O-Si bond of the glass powder. The broadbands at 781 cm^{-1}, 464 cm^{-1} are due to the vibrations of the Ti-O bond at all the samples M0, M4, M8. The shoulder at 935 cm^{-1} is indicated of the bond of Ti-O-Si, that mean TiO_2 is bonded with SiO_2 in the glass sample [17].

3.4. SEM and SEM-EDX images of the coating on the surface of glass plate

On the SEM images (Fig. 5) it is quite clearly seen the dissolution. creating geopolymer of the sample with the ratio of FA / (WS+FA) = 40 %. This sample was selected for SEM analysis because of its highest mechanical strength showing the ability to create good polymerization.

The SEM images (Fig. 5a) and the EDS images (Fig. 5b) of the coating of M8 on the surface of a glass plate are shown in the figure. The sample used for SEM was not coated by noble metals like Au, Pt to detect Ag in this one. The compositions of elements at two different points (a and b) are shown in Table 3.

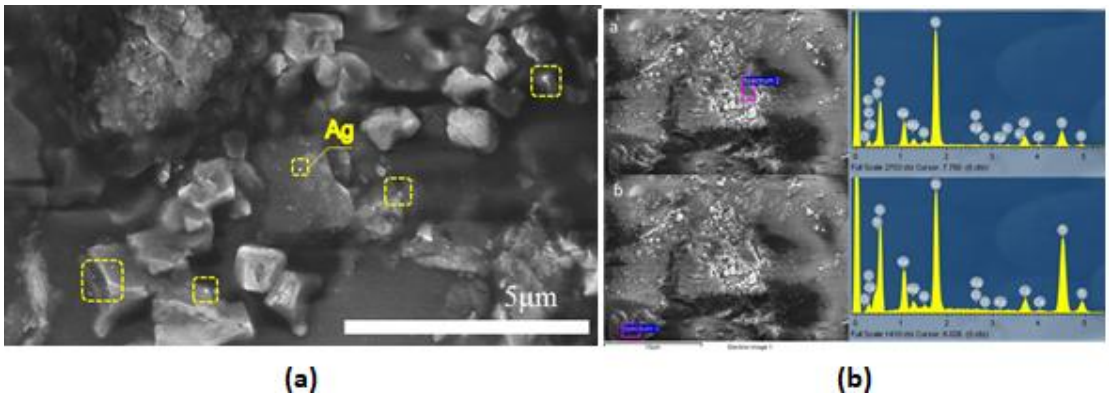

Figure 5. SEM (a) and EDS (b) images of the coating M8 on the surface of a glass plate.

In Figure 5a, anatase crystals with a size of about 1 – 2 µm can be seen quite clearly. The bright dots may be clusters of Ag particles on the crystal surface of TiO_2. This phenomenon is seen on the SEM images of the coating M8. The EDS spectrum and the data in Table 3 confirm the presence of primary elements of Ti, Ag, and O of the coating. Other elements such as Si, Na, Al, Ca, etc. are elements in the glass composition. The element C of organic substance has not yet decomposed.

Table 3. The compositions (% wt.) of elements at two different points (a and b).

Point	C	O	Na	Mg	Al	Si	Cl	K	Ca	Ti	Ag
a	11.20	54.60	6.18	1.16	0.54	19.40	0.14	0.13	2.18	4.46	0.01
b	10.05	60.44	6.17	0.79	0.23	10.04	0.13	-	0.17	10.94	0.04

3.5. The photocatalytic ability

The degradation efficiency of MB was used to test for photocatalytic ability. Two samples M2 and M6 have been prepared to clarify the results. The degradation efficiency of the samples M0, M2, M4, M6, M8 under an UV lamp 50 W for 2 hours is shown in Figure 6a. The photocatalytic-degradation solution was analyzed by a UV-Vis spectroscopy. The results indicated that the MB solutions were absorbed and decomposed in all samples. However, the sample M4 has the highest photocatalytic ability. The photocatalytic ability of M4 with M0 by determining the concentration reduction (ppm) of 50 mL MB 5 ppm solution with M4 and M0 under the UV lamp 50 W in intervals of time (min.): 0; 30; 60; 90; 120 was compared. The results are shown in Figure 6b.

Reuse of the material: After being tested, the M4 sample was exposed to the sun, washed and then repeated the test "The decomposition efficiency of MB". The reused samples still have the efficiency of 61.2 %, approximate to the original material (61.4 %).

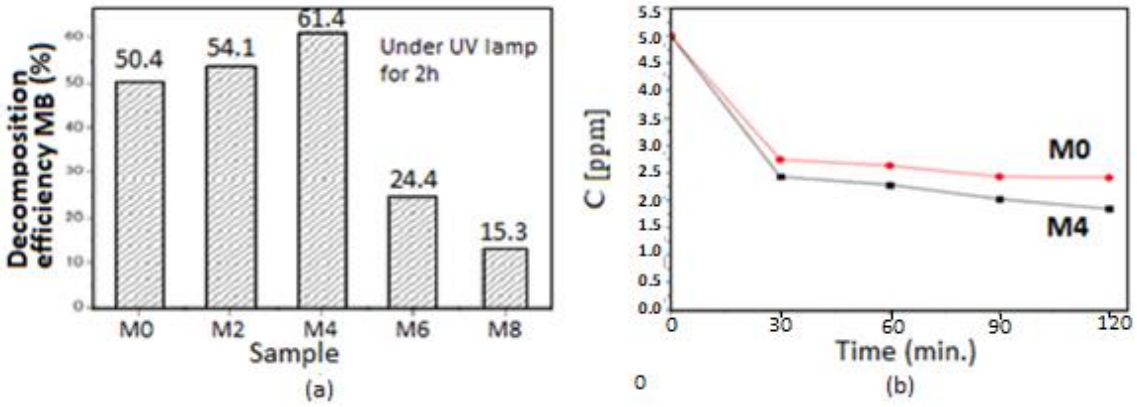

Figure 6. The decomposition efficiency of MB (a) and compare the photocatalytic ability of M4 with M0 (b).

3.6. The antibacterial ability

The results of antibacterial ability of the samples against *E. coli* bacteria are shown in Table 4 and Figure 7. According to experimental results, only the sample M4 and only when content greater than 2.00 mg/mL had the antibacterial ability.

Table 4. The results against *E.coli* bacteria. (+): bacteria (-): no bacteria.

Sample	Concentration (mg/mL)									
M4	16.00	8.00	4.00	2.00	1.00	0.50	0.25	0.125	0.063	0.031
	-	-	-	-	+	+	+	+	+	+
Reference	+									

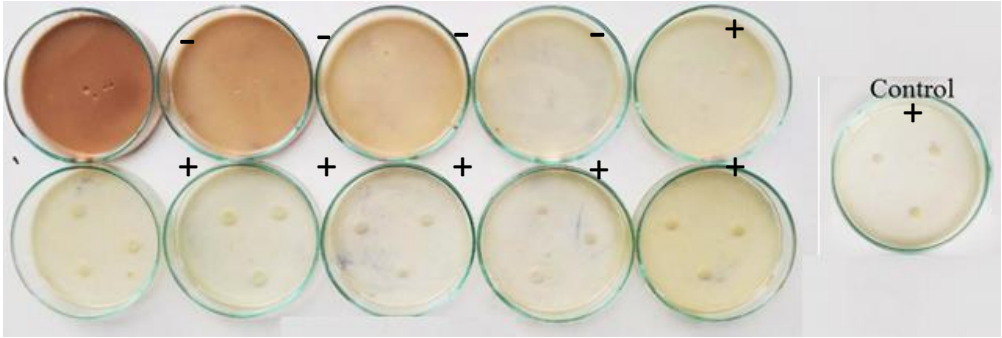

Figure 7. The results against *E.coli* bacteria of the antibacterial agent in Mueller-Hinton agar plates.

4. CONCLUSION

The Ag/TiO_2 composite was synthesized by thermal decomposition at 570 ^oC for 1 hour of the solution of the Ag resinate from the coconut oil and the TBO in the commercial solvent C8720. This is the heating temperature that ensures inorganic substances create a solid coating on the glass surface. The Ag/TiO_2 composite formation and its microstructure were confirmed by XRD, FTIR spectra, SEM images, and EDS analysis. It was observed that the crystalline phase of TiO_2 was anatase and Ag dispersed in the matrix of TiO_2 or may be partially replaced in the crystal structure. The change of lattice parameters and reduction E_g represents the replacement of Ag in the structure of TiO_2 crystals.

The photocatalytic ability of glass powder with the Ag/TiO_2 coating was investigated by the MB photo degradation. The reduction of Eg has increased the range of the visible light effect and the photocatalytic ability [18]. But when Ag content increases, the Ag particles will be agglomerated and cover on the TiO_2 surface to prevent sunlight / UV rays, so the photocatalytic ability of TiO_2 will be decreased [18, 19]. In our experiments the ratio of Ag/TiO_2 = 4 % mol. is considered optimal for photocatalytic ability. At the same time, the Ag/TiO_2 composite was shown the antibacterial effect *E.coli* when the content of Ag greater than 4 %.

REFERENCES

1. Sobana N., Muruganadham M., and Swaminathan M. - Nano-Ag particles doped TiO_2 for efficient photodegradation of Direct azo dyes, J. Mol. Catal. **258** (1-2) (2006) 124-132.

2. Ali T., Ahmed A., and Alam U. - Enhanced photocatalytic and antibacterial activities of Ag-doped TiO_2 nanoparticles under visible light, Mater. Chem. Phys. **212** (2018) 325-335.
3. Dong P. T. and Byeong-Kyu L. - Effects of Ag doping on the photocatalytic disinfection of E. coli in bioaerosol by Ag–TiO_2/GF under visible light, J. Colloid Interface Sci. **428** (2014) 24–31.
4. Avciata O., Benli Y., and Gorduk S. - Ag doped TiO_2 nanoparticles prepared by hydrothermal method and coating of the nanoparticles on the ceramic pellets for photocatalytic study: Surface properties and photoactivity, J. Eng. Technol. Appl. Sci. **1** (2016) 22-26.
5. Avciataa O., Benli Y., Gordukb S., and Koyunb O. - Ag doped TiO_2 nanoparticles prepared by hydrothermal method and coating of the nanoparticles on the ceramic pellets for photocatalytic study: surface properties and photoactivity, Journal of Engineering Technology and Applied Sciences **1** (1) (2016) 34-50.
6. Nhu V. T. T., Minh D. Q., Duy N. N., and Hien N. Q. - Photocatalytic Degradation of Azo Dye (Methyl Red) In Water under Visible Light Using Ag- Ni/TiO2 Sythesized by β - Irradiation Method - International Journal of Environment, Agriculture and Biotechnolog **2** (2017) 529 – 538.
7. Mogal S. I., Gandhi V. G., Mishra M., Tripathi S., Shripathi T., Joshi P. A., and Shah Di. O. - Single-Step Synthesis of Silver-Doped Titanium Dioxide: Influence of Silver on Structural, Textural, and Photocatalytic Properties, Industrial & Engineering Chemistry Research **53** (2014) 5749 – 5958.
8. Chao H. E., Yun Y. U., and Xingfang H. U. - Effect of silver doping on the phase transformation and grain growth of sol-gel titania powder, J. Eur. Ceram. Soc. **23** (2003) 1457–1464.
9. Trevizo A. S., Madrid P. A., Piza P., Antunez W., and Yoshida M. M. - Optical Band Gap Estimation of ZnO Nanorods, Mater. Res. Ibero-Am. J. Mater. **19** (2016) 1-5.
10. Larkin P. - IR and Raman Spectroscopy: Principles and Spectral Interpretation – Elsevier, 2011.
11. Ashtari M., Ortega L. C., Linares F. L., Eldood A., and Almao P. P. - New Pathways for Asphaltenes Upgrading Using the Oxy-Cracking Process, Energy Fuels **30** (6) (2016) 4596–4608.
12. Duhan S. - Microstructure and Surface Morphology of Nanocrystalline Silver Silicates – Acta Physica Polonica **121** (3) (2012) 636-638.
13. Shameli K., Ahmad M. B., and Davoud J. S. - Synthesis and Characterization of Polyethylene Glycol Mediated Silver Nanoparticles by the Green Method, Int. J. Mol. Sci. **13** (6) 2013 6639-6650.
14. "Anatase R060277 - RRUFF Database: Raman, X-ray, Infrared, and Chemistry." [Online]. Available: http://rruff.info/anatase/display=default/R060277. [Accessed: 25-May-2019].
15. "Rutile R110109 - RRUFF Database: Raman, X-ray, Infrared, and Chemistry." [Online]. Available: http://rruff.info/rutile/display=default/R110109. [Accessed: 25-May-2019].
16. "Silver R070463 - RRUFF Database: Raman, X-ray, Infrared, and Chemistry." [Online]. Available: http://rruff.info/silver/chem=Ag/display=default/R070463. [Accessed: 25-May-2019].

17. Kim W. B. - Quantitative Analysis of Ti−O−Si and Ti−O−Ti Bonds in Ti−Si Binary Oxides by the Linear Combination of XANES - The Journal of Physical Chemistry B **104** (36) (2000) 8670-8678.
18. Dong P. T., and Kyu L. B. - Effects of Ag doping on the photocatalytic disinfection of E. coli in bioaerosol by Ag–TiO2/GF under visible light, J. Colloid Interface Sci. **428** (2014) 24–31.

Mogal S. I., Gandhi V. G., Mishra M., and Tripathi S. - Single-Step Synthesis of Silver-Doped Titanium Dioxide: Influence of Silver on Structural, Textural, and Photocatalytic Properties, Am. Chem. Soc. **53** (2014) 5749−5758.